Acta Crystallographica Section D
Biological Crystallography
ISSN 0907-4449

Expression, purification, crystallization and preliminary X-ray crystallographic studies of *Mycobacterium tuberculosis* thioredoxin reductase

Mohd Akif, Radha Chauhan and Shekhar C. Mande*

Centre For DNA Fingerprinting and Diagnostics, Hyderabad, India

Correspondence e-mail: shekhar@cdfd.org.in

Received 27 January 2004
Accepted 25 February 2004

Mycobacterium tuberculosis (H37Rv), the causative agent of the dreaded disease tuberculosis, contains three thioredoxins and a single thioredoxin reductase. Thioredoxin reductase is a member of the pyridine-nucleotide disulfide oxidoreductase family of flavoenzymes. The thioredoxin reductase gene with a His tag at the C-terminus was expressed in *Escherichia coli* and purified. The dimeric (70 kDa) protein was incubated with 10 m*M* DTT for 30 min and then crystallized using the hanging-drop vapour-diffusion method in the presence of 15% PEG 3350 and phosphate–citrate buffer pH 5 at room temperature (298 K). A diffraction data set complete to 3 Å resolution has been collected under cryoconditions and the space group was determined to be $P4_12_12$, with unit-cell parameters $a = 107.4$, $c = 118.2$ Å. Matthews coefficient calculations revealed the presence of two monomers in the asymmetric unit.

1. Introduction

Mycobacterium tuberculosis (H37Rv) has infected more than one third of the world's population (Dolin *et al.*, 1994). *M. tuberculosis* spends much of its life cycle in the strong oxidative environment of macrophages and therefore requires effective oxidative stress defences (Schorey *et al.*, 1997). The thioredoxin system is a key player in the oxidative-defence system of the cell and helps in its survival in the presence of oxidative stress (Takemoto *et al.*, 1998). Reactive oxygen species have many harmful effects on cells. For example, they can oxidize cysteine residues, leading to the formation of undesirable disulfide bridges. Such reactions often inactivate cellular proteins. Reduction of these products may be accomplished in microbial systems by the thioredoxin/thioredoxin reductase (TrxR; Farr & Kogoma, 1991) or glutathione/glutathione reductase systems. In addition to this, in many organisms peroxiredoxins catalyse the reduction of peroxides and thereby prevent oxidative stress and the induction of apoptosis. Peroxiredoxins require reduction by thioredoxin and thioredoxin reductase (Chae *et al.*, 1999). TrxR is a flavoprotein that catalyses the reduction of Trx by NADPH (Moore *et al.*, 1964; Williams, 1995). The substrate Trx in its dithiol state plays a key role in maintaining the redox environment of the cell (Holmgren, 1989). *M. tuberculosis* has three Trx genes and a single TrxR-encoding gene and surprisingly no glutathione/glutathione reductase-encoding genes in its genome sequence (Cole *et al.*, 1998). In the absence of a glutathione/glutathione reductase system, the thioredoxin/thioredoxin reductase system is obviously critical for this mycobacterium to maintain its intracellular redox environment. In order to determine the three-dimensional structure of mycobacterial TrxR, we have crystallized *M. tuberculosis* thioredoxin reductase (TrxR). This paper describes the preliminary crystallographic characterization of the mycobacterial TrxR crystals.

2. Material and methods

2.1. Expression and purification

BACRv13 cosmid DNA of *M. tuberculosis* (H37Rv), kindly provided by Stewart Cole, was used as a template for PCR amplification of the 1005 bp *trxR* gene (Rv3913). The forward primer 5′-TTATTCCATATGACCGCCCCG-CCTCTCCA-3′ and the reverse primer 5′-AACTAAGCTTTCAGTGGTGGTGGT-GGTGGTGTCGTTGTGCTCCTATCAAT-3′ were designed to contain a start-site codon and codons for six histidines, respectively. The PCR product was ligated into the pET23a (Novagene) expression vector using *Nde*I and *Hin*dIII restriction-endonuclease sites. The cloned gene sequence was confirmed by automated DNA sequencing. The plasmid harbouring the mycobacterial *trxR* gene was transformed into the *Escherichia coli* BL21 (DE3) expression system and the recombinant protein was purified using Ni^{2+}–nitrilotriacetate (NTA) chromatography. Briefly, cells were grown in Terrific broth at 310 K until they reached an OD_{600} of 0.6 and were then induced with 1 m*M* isopropyl β-D-thiogalactoside. The cells were lysed by sonication and centrifuged at 13 000 rev min^{-1} for 20 min at 277 K. The supernatant was loaded onto an Ni^{2+}–NTA

column. The column was washed with 50 m*M* phosphate buffer pH 8 containing 300 m*M* NaCl, 5% glycerol and 20 m*M* imidazole. The protein was eluted with the same buffer supplemented with 250 m*M* imidazole. The purity was checked on Coomassie-stained SDS–PAGE, where it appeared as a single band (Fig. 1).

2.2. Crystallization

The purified protein was dialyzed against 10 m*M* Tris–HCl pH 8.0 buffer and then concentrated to 30 mg ml^{-1}. Before crystallization, 10 m*M* reduced DTT was added to the protein solution and the solution was incubated for 30 min on ice. Initial crystallization trials were performed using a random screening of chemical conditions in our laboratory. The screening was conducted using the hanging-drop vapour-diffusion technique in 24-well plates. A 2 µl droplet of protein mixed in a 1:1 ratio with reservoir solution was equilibrated against 500 µl reservoir solution at room temperature. Crystals suitable for X-ray diffraction (Fig. 2) were obtained using 0.1 *M* sodium phosphate–citrate buffer pH 5.0 and 15% PEG 3350 at room temperature. Crystals grew within 36 h to dimensions of 0.5 × 0.5 × 0.3 mm.

2.3. X-ray data collection and processing

Crystals were soaked in cryoprotectant solution for a few seconds prior to freezing in a nitrogen cold stream. The cryoprotectant solution contained 11% ethylene glycol, 20% PEG 3350 and 0.1 *M* sodium phosphate–citrate buffer pH 5.0. X-ray diffraction data were collected at 100 K on beamline XRD-1 (wavelength = 0.927 Å) at the ELETTRA synchrotron facility, Trieste, Italy using a MAR CCD 165 detector. The crystal-to-detector distance was maintained at 200 mm with an oscillation range per image of 1°, covering a total oscillation range of 100° (Fig. 3). Determination of the unit-cell parameters and integration of reflections were performed using the programs *DENZO*/*SCALEPACK* (Otwinowski & Minor, 1997). The intensities were then converted to the corresponding structure-factor amplitudes using the *TRUNCATE* program from the *CCP*4 suite (Collaborative Computational Project, Number 4, 1994).

Molecular replacement was attempted using the *AMoRe* program (Navaza, 1994) from the *CCP*4 suite. The homologous *E. coli* TrxR (dimeric) crystal structure (PDB code 1tde), which has 46% sequence identity (Waksman *et al.*, 1994), was used as the search model.

3. Results and discussion

The *trxR* gene encoding a polypeptide of 335 amino acids was cloned and expressed in *E. coli* and the protein was purified to homogeneity. The protein purity was observed to be better than 98% as shown in Fig. 1. On gel-filtration chromatography, the purified TrxR protein eluted in a dimeric form, which is consistent with the physiological quaternary state of the *E. coli* TrxR (Moore *et al.*, 1964; Russel & Model, 1988) (data not shown). Crystallization trials using the mycobacterial TrxR yielded bright yellow coloured crystals (Fig. 2) of dimensions ~0.5 × 0.5 × 0.3 mm. These crystals were not stable when data collection was attempted at room temperature. However, the crystals appeared to be comparatively stable under cryoconditions. Diffraction data were collected at the ELETTRA synchrotron source, Italy in the presence of the cryoprotectant ethylene glycol. The completeness of the data set was found to be 97.8% with acceptable statistical parameters. The 3 Å resolution data were processed using the *HKL*2000 program and the space group was determined to be $P4_x2_x2$, with unit-cell parameters a = 107.4, c = 118.2 Å. Analysis of the systematic absences was not conclusive because only a few reflections of the relevant form were present. The $R_{\rm merge}$ values increased rapidly beyond 3 Å resolution and hence data were only processed to 3 Å resolution. Assuming the presence of two monomers in the asymmetric unit, a value for the Matthews coefficient of 2.5 Å^3 Da^{-1} was obtained, which corresponds to a solvent content of 51.4% (Matthews, 1968). Data-collection and resolution statistics are shown in Table 1. The self-rotation function plot did not show any peaks for the expected twofold noncrystallographic symmetry. The Patterson calculated using native intensities also did not show any significant peak apart from the origin, ruling out the possibility of pseudo-translation. The $N(Z)$ test and the $\langle I^2\rangle/\langle I\rangle^2$

Table 1
Data-collection statistics.

Values in parentheses refer to the last resolution shell (3.11–3.0 Å).

Wavelength (Å)	0.927
Space group	$P4_12_12$
Unit-cell parameters (Å)	a = 107.4, c = 118.2
Resolution limits (Å)	50.0–3.0
Unique reflections	14186 (1368)
$I/\sigma(I)$	16.2 (4.1)
$R_{\rm merge}$† (%)	8.1 (36.9)
Completeness (%)	97.8 (97.9)
Probable solvent content (%)	51.4
No. molecules in AU	2
Matthews coefficient (Å^3 Da^{-1})	2.5

† $R_{\rm merge} = \sum_{hkl}\sum_i |I_i(hkl) - \langle I(hkl)\rangle| / \sum_{hkl}\sum_i I_i(hkl)$, where $I_i(hkl)$ are the intensities of symmetry-redundant reflections and $\langle I(hkl)\rangle$ is the average intensity over all observations.

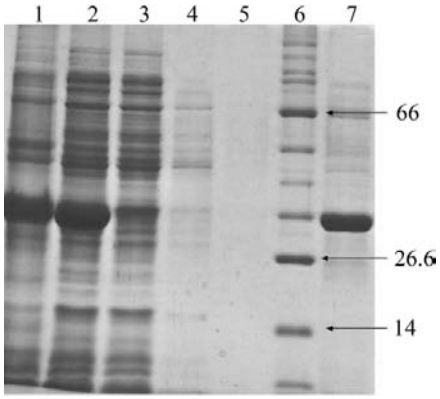

Figure 1
10% SDS–PAGE gel showing protein purification. Lane 1, cell supernatant after sonication; lane 2, flowthrough; lanes 3, 4 and 5, washthrough from Ni^{2+}–NTA column; lane 6, molecular-weight markers (kDa); lane 7, purified TrxR.

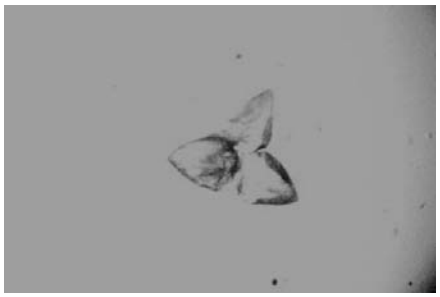

Figure 2
A crystal of reduced TrxR grown using 15% PEG 3350 and 0.1 *M* sodium–phosphate citrate pH 5.0. The size of one of the crystals shown is approximately 0.5 × 0.5 × 0.3 mm.

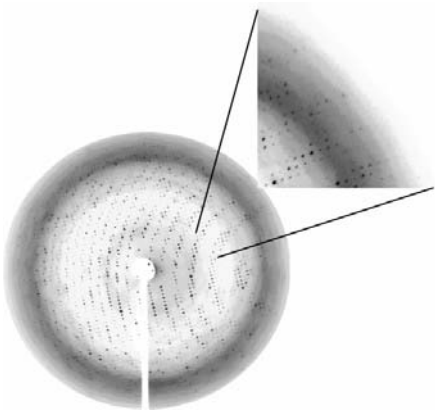

Figure 3
A 1° oscillation image collected at the ELETTRA synchrotron at 100 K temperature from a native TrxR crystal. The inset clearly shows the presence of reflections beyond the solvent ring.

distribution clearly indicated that the intensity data were not twinned.

The *AMoRe* (Navaza, 1994) program was used for molecular-replacement calculations using *E. coli* dimeric TrxR (PDB code 1tde) as the search model. The screw axes of the space group (which could not be identified earlier) were determined during translation searches in *AMoRe*. The best molecular-replacement solution was obtained in space group $P4_12_12$. The correctly oriented and positioned molecule of TrxR showed a correlation coefficient of 64.2 and an *R* factor of 47.5%. In comparison, the next best solution showed a correlation coefficient of 47.1 and an *R* factor of 55.1%. The placement of the model using the molecular-replacement solution did not show any unfavourable overlaps between symmetry-related molecules.

Currently, refinement of the molecular-replacement solution is in progress. The crystal structure of *M. tuberculosis* TrxR will contribute to the rational design of inhibitors. The structure will also increase the understanding of the catalytic mechanisms of Trx/TrxR in *M. tuberculosis*.

We thank Stewart Cole and colleagues for providing a cosmid DNA library of *M. tuberculosis* H37Rv. We also thank the staff of the XRD1 beamline at the ELETTRA synchrotron, Trieste, Italy for assistance during data collection and ICTP for financial assistance in performing experiments at ELETTRA. We thank Howard Einspahr for useful suggestions. This work is supported by grants from the Department of Biotechnology and the Council of Scientific and Industrial Research (CSIR), New Delhi, India. MA gratefully acknowledges financial support from the CSIR for a Junior Research Fellowship and RC and SCM that from the Wellcome Trust, UK.

References

Chae, H. Z., Kang, S. W. & Rhee, S. G. (1999). *Methods Enzymol.* **300**, 219–226.
Cole, S. T. *et al.* (1998). *Nature (London)*, **393**, 537–544.
Collaborative Computational Project, Number 4 (1994). *Acta Cryst.* D**50**, 760–763.
Dolin, P. J., Raviglion, M. C. & Kohi, A. (1994). *Bull. World Health Org.* **72**, 213–220.
Farr, S. B. & Kogoma, T. (1991). *Microbiol. Rev.* **55**, 561–585.
Holmgren, A. (1989). *J. Biol. Chem.* **264**, 13963–13966.
Matthews, B. W. (1968). *J. Mol. Biol.* **33**, 491–497.
Moore, E. C., Reichard, P. & Thelander, L. (1964). *J. Biol. Chem.* **239**, 3445–3452.
Navaza, J. (1994). *Acta Cryst.* A**50**, 157–163.
Otwinowski, Z. & Minor, W. (1997). *Methods Enzymol.* **276**, 307–326.
Russel, M. & Model, P. (1988). *J. Biol. Chem.* **263**, 9015–9019.
Schorey, J. S., Carroll, M. C. & Brown, E. J. (1997). *Science*, **277**, 1091–1093.
Takemoto, T., Zhang, Q. M. & Yonei, S. (1998). *Free Radic. Biol. Med.* **24**, 556–562.
Waksman, G., Krishna, T. S. R., Williams, C. H. Jr & Kuriyan, J. (1994). *J. Mol. Biol.* **236**, 800–816.
Williams, C. H. Jr (1995). *FASEB J.* **9**, 1267–1276.